Perturbation of Hyaluronan Synthesis in the Trabecular Meshwork and the Effects on Outflow Facility

Kate E. Keller, Ying Ying Sun, Yong-Feng Yang, John M. Bradley, and Ted S. Acott

Purpose. Hyaluronan (HA) is a major component of the aqueous outflow pathway. However, the contribution of HA to human outflow resistance remains unclear. Three HA synthase genes (HAS1-3) have been identified. Here, we evaluate the contribution of each of the HAS proteins to outflow facility in anterior segment perfusion culture.

Methods. Two methods were used to reduce HA synthesis: 1 mM 4-methylumbelliferone (4MU) was used to inhibit all HAS synthases and shRNA silencing lentivirus was generated to knock down expression of each HAS individually. Quantitative RT-PCR, Western immunoblotting and an HA ELISA assay were used to assess HAS mRNA and protein levels and HA concentration, respectively. The effects of 4MU treatment and HAS gene silencing on outflow facility were assessed in human and porcine perfusion culture.

Results. Quantitative RT-PCR and Western immunoblotting showed a reduction of each HAS in response to their respective silencing and 4MU treatment. HA concentration was concomitantly reduced. Treatment with 4MU decreased outflow facility in human anterior segments but increased outflow facility in porcine eyes. Lentiviral delivery of HAS1 and HAS2 silencing vectors caused similar opposite effects on outflow facility. Silencing of HAS3 did not significantly affect outflow resistance in either species.

Conclusions. This is the first conclusive evidence for a significant role of HA in the human outflow pathway. HA chains synthesized by HAS1 and HAS2 contribute to outflow resistance, while hyaluronan produced by HAS3 does not appear to play a significant role. (*Invest Ophthalmol Vis Sci.* 2012;53:4616–4625) DOI:10.1167/iovs.12-9500

Hyaluronan (HA) is a large, negatively charged glycosaminoglycan (GAG) chain that is synthesized by three homologous hyaluronan synthase (HAS) enzymes called HAS1, HAS2 and HAS3.[1–5] In contrast to all other GAG chains, which are synthesized directly on proteoglycan core proteins in the endoplasmic reticulum and Golgi, HA is synthesized at the cell surface.[2] The growing HA chain is extruded directly through the plasma membrane into the extracellular milieu. As a result, HA is not sulfated and does not undergo epimerization. Each HAS produces HA in differing amounts and of different sizes: HAS1 produces low amounts of high molecular weight (HMW) HA, HAS2 produces high amounts of HMW HA, while HAS3 produces high amounts of low MW (LMW) HA.[5] The coumarin derivative, 4-methylumbelliferone (4MU), is a potent inhibitor of HA synthesis and exerts its effects two ways: it decreases HAS2 and HAS3 mRNA levels and also depletes the cellular pool of UDP-glucuronic acid, a building block of HA chains.[6] Subsequent studies suggest that 4MU also decreases HAS1 mRNA levels.[7] Previous studies have shown that HASs are expressed by bovine trabecular meshwork cells and in primate trabecular meshwork tissue.[8,9]

In the trabecular meshwork (TM), HA represents approximately 20% to 25% of the total GAGs.[10] HA distribution in the TM has been assessed using HA binding protein (HAbp). HA was found in the anterior non-filtering portion of the TM and in the juxtacanalicular (JCT) or cribriform region near the inner wall of Schlemm's canal.[11–14] This is the region implicated in generating outflow resistance.[15,16] At the ultrastructural level, HAbp staining in the JCT was found abundantly in the core and sheaths of sheath-derived plaques, with less staining in the amorphous basement-membrane-like materials.[17] It has been postulated that HA covering the surfaces of the outflow pathways might prevent adherence of debris and aqueous humor components to ECM molecules and prevent clogging of the outflow pathways.[14,18] As humans age, there is a decrease in the amount of HA and there is a much greater loss in primary open-angle glaucoma (POAG) TM.[12,19,20] This loss is most pronounced in the JCT region.[12] Experiments performed in the 1950's demonstrated that treatment of bovine eyes with hyaluronidase to degrade HA decreased outflow resistance and consequently increased outflow facility.[21] These results were replicated in many animal species,[22–25] but experiments using primate and human eyes were inconclusive.[26–28] Together, these expression and degradation studies argue for a primary role of HA in outflow resistance, although the contribution of HA to human aqueous outflow remains unclear.

Recently, we showed that RNAi silencing of versican, an HA binding protein, reduced outflow facility in human anterior segment perfusion culture.[29] Histopathologic analysis of TM sections post-silencing showed that there was an accumulation of hyaluronidase-sensitive material in the JCT region. This suggests that disruption of HA networks may have partially contributed to the observed effect of versican silencing on outflow facility. In this study, we further investigate the role of HA in outflow facility by reducing HA levels in the TM by either 4MU treatment or by knocking down expression of each individual HAS gene using RNAi silencing. The morphology of the TM following HAS knockdown and 4MU treatment was assessed.

From the Casey Eye Institute, Oregon Health & Science University, Portland, Oregon.

Supported by National Institutes of Health Grants EY019643 (KEK), EY003279, EY008247, EY010572 (TSA); a Shaffer Award for Innovative Research from the Glaucoma Research Foundation, San Francisco, California (KEK); Fight for Sight, New York, New York (KEK); and by an unrestricted grant to the Casey Eye Institute from Research to Prevent Blindness, New York, New York.

Submitted for publication January 13, 2012; revised May 16, 2012; accepted June 6, 2012.

Disclosure: **K.E. Keller**, None; **Y.Y. Sun**, None; **Y.-F. Yang**, None; **J.M. Bradley**, None; **T.S. Acott**, None

Corresponding author: Kate E. Keller, Casey Eye Institute, Oregon Health & Science University, 3181 SW Sam Jackson Park Road, Portland, OR 97239; gregorka@ohsu.edu.

Investigative Ophthalmology & Visual Science, July 2012, Vol. 53, No. 8

Materials and Methods

Generation of HAS Gene shRNA Silencing Lentivirus

Short, hairpin RNA (shRNA) vectors were generated in order to silence, individually, each of the three HAS genes (shHAS1-3) as previously described for versican and ASB10.[29,30] Briefly, shRNAs were designed using the online BLOCK-iT RNAi designer (Invitrogen, Carlsbad, CA). A shRNA control (shCtrl) was also designed that did not target any other known human or porcine gene when blasted against the NCBI database. The sequences of the silencing primers were:

HAS1:	5′-CACCGGTCATGTACACCGCCTTCAACGAATT GAAGGCGGTGTACATGACC-3′
HAS2:	5′-CACCGGGACGAAGTGTGGATTATGTCGAAA CATAATCCACACTTCGTCCC-3′
HAS3 (human):	5′-CACCGCATTATCAAGGCCACCTACGCGAACG TAGGTGGCCTTGATAATGC-3′
HAS3 (pig):	5′-CACCGCTGGAGCAAGTCTTACTTCCCGAAG GAAGTAAGACTTGCTCCAGC-3′
Control:	5′-CACCCATCACTCCATGTTGGAACTTC GAAAAGTTCCAACATGGAGTGATG-3′

Double-stranded shRNAs were generated, cloned into the pENTR/U6 vector using T4 ligase (Invitrogen) and the sequences were verified by DNA sequencing. The shRNA cassette was transferred into the pLenti6/BLOCK-iT-DEST vector (HIV-based lentiviral vector) by recombination. To generate replication incompetent lentivirus, 3 μg of pLenti silencing plasmid was co-transfected with 9 μg ViraPower packaging mix (Invitrogen) into 293FT cells using Lipofectamine 2000 (Invitrogen). Lentiviral-containing supernatants were harvested 72 hours post-transfection. Viral titers were determined by infecting HT1080 cells and the multiplicity of infection was calculated in plaque formation units (pfus).[29,30]

Quantitative RT-PCR

Primary TM cells were isolated from TMs dissected from human donor eyes or porcine eyes.[31,32] TM cells were infected with 10^6 pfus of shHAS lentivirus in the presence of 6 μg/mL polybrene (Sigma, St. Louis, MO) at the time of plating and cultured for 72 hours. For 4MU treatments, TM cells were grown to confluence and then treated with various concentrations (0, 0.5, 1 and 2 mM) of 4MU in dimethylsulfoxide (DMSO) in serum-free Dulbecco's modified Eagle's medium (DMEM) for 24 hours. Control cells were treated with a 1:1000 dilution of DMSO. For both treatments, total RNA was isolated using cells-to-cDNA lysis buffer (Ambion, Austin, TX) and cDNA was generated using Superscript III reverse transcriptase (Invitrogen). Gene knockdown was verified using quantitative RT-PCR (qRT-PCR) with HAS1, HAS2 or HAS3 specific primers and methods described previously.[33,34] Results were normalized to 18S RNA, which acted as a housekeeping gene, and expressed as a percentage of the vehicle control or shCtrl-infected TM cells.

Western Immunoblotting

For Western immunoblotting, RIPA lysates were harvested from porcine or human TM cells treated with 1 mM 4MU or vehicle control for 3 days, or from TM cells infected with the individual HAS silencing lentivirus. For infection, approximately 10^6 pfus silencing lentivirus were added to the media at the time of plating with 6 μg/mL polybrene. TM cells were infected for 6 days, cells and ECM were scraped into RIPA buffer and 30 μL of RIPA lysate was loaded into each lane. Proteins were separated on 10% SDS-PAGE gels (BioRad Labs, Hercules, CA) under reducing conditions and transferred to nitrocellulose. Primary antibodies were a monoclonal anti-HAS1 (Novus Biologicals, Littleton, CO), a goat anti-HAS2 polyclonal (Santa Cruz Biotechnology, Inc., Santa Cruz, CA) and a rabbit anti-HAS3 polyclonal (Abcam, Cambridge, MA). Secondary antibodies were IRDye 700-conjugated anti-rabbit and IRDye 800-conjugated anti-mouse or anti-goat (Rockland Immunochemicals, Gilbertsville, PA). Western immunoblots were imaged using the Odyssey infrared imaging system (Licor, Lincoln, NE). Bands were quantitated using Image J software following background correction and values were then normalized to actin as a loading control. There was no significant difference in actin levels or total protein levels, as quantitated by a BCA assay (Pierce, Rockford, IL), between treatments and controls. Average pixel intensity was determined from 3 independent experiments.

HA ELISA Assay

To ensure that HA levels were reduced by 4MU treatment and shHAS gene silencing, an HA ELISA assay was performed. Confluent human or porcine TM cells were treated with 1 mM 4MU for 24 hours in serum-free DMEM, or were infected with 10^6 pfus of shHAS lentivirus for 72 hours. The infected cells were washed in PBS and serum-free DMEM was added for a further 24 hours. Media was harvested and the cells and extracellular matrix (ECM) were scraped into RIPA buffer on ice. HA levels in media and RIPA lysates were quantitated using a competitive HA ELISA kit following the manufacturer's instructions (Echelon Bioscience, Salt Lake City, UT). HA levels in ng/mL were calculated from a standard HA curve run on each plate. Each sample was tested in triplicate, individual results were averaged and a percentage of the control was calculated. At least three independent experiments were performed for each treatment.

Perfusion of Anterior Segments

Human donor eye pairs were acquired from Lions Eye Bank of Oregon (Portland, OR) within 24 to 48 hours of death. The average age of donor eyes was 83.27 ± 1.358 years, age range 67 to 92. All anterior segments were placed into serum-free stationary organ culture for 5 to 7 days prior to perfusion culture to allow for cellular recovery. Human donor tissue protocols were approved by the Oregon Health & Science University Institutional Review Board and were conducted in accordance to the tenets of the Declaration of Helsinki. Porcine eyes were acquired from the local slaughterhouse and placed into perfusion culture within 4 hours of death. Anterior segments from human and porcine eyes were perfused at constant pressure (8.8 mmHg) with serum-free media until flow rates stabilized at an average flow rate of 1 to 7 μL/min for humans and 2 to 8 μL for porcine eyes.[29,34–36] Any eyes that could not be stabilized at these flow rates were discarded. Lentivirus (10^8 pfu) was applied as a bolus to the perfusion chambers by media exchange (indicated by time point 0) and outflow facility was measured for a further 3 to 7 days. For 4MU treatment, serum-free media containing 1 mM 4MU or dimethyl sulfoxide (DMSO) vehicle (control) was perfused for the entire duration of the experiment. For both treatments, change in outflow facility was determined by dividing flow rate after treatment by the average outflow rates prior to treatment. Data from individual eyes were then combined and averaged.

At the end of the experiment, anterior segments were removed from the perfusion chambers and either fixed in 4% paraformaldehyde for immunofluorescence and confocal analysis, or the TM's were removed by dissection and RNA was isolated using TRIzol (Invitrogen). qRT-PCR was used to determine the efficacy of knockdown of HAS genes following perfusion as described above. For immunohistochemistry studies, anterior segments were cut into approximately 6 to 8 wedges, each of which were embedded in a single paraffin block. Five μm serial radial sections were cut approximately perpendicular to Schlemm's canal at the pathology/histology core facility of the Knight Cancer Institute (Oregon Health & Science University, Portland, OR).[35] To assess HA distribution in the TM, biotinylated HA binding protein (bHAbp) was used (EMD Biosciences, San Diego, CA). Sections were deparaffinized, blocked and 10 μg/mL bHAbp was incubated overnight at 4°C.[37] bHAbp was detected with AlexaFluor 594nm-conjugated Streptavidin (Invitrogen). Coverslips were mounted in ProLong gold

containing DAPI nuclear stain (Invitrogen) and tissue sections were visualized with a Fluoview laser confocal scanning microscope (Olympus, San Diego, CA) with associated software. Some sections were stained with hematoxylin and eosin (H&E).

Statistical Analyses

Data are presented as the mean ± standard error of the mean. The "*n*" for each experiment is noted in the figure, or in the text accompanying each figure. An unpaired Student's *t*-test or one-way analysis of variance (ANOVA) was used to determine significance. To account for multiple comparisons, Bonferroni's post hoc correction was applied. To determine significance of proportions, a two-tailed Fisher exact test was performed. A *P*-value < 0.05 was considered significant.

Results

4MU Treatment and shHAS Silencing in TM Cells

HAS mRNA levels were quantitated in response to various doses of 4MU in TM cells (Fig. 1). By qRT-PCR, the mRNAs for all three HASs were significantly reduced by 4MU treatment at 24 hours ($P < 0.05$). To verify there was a concomitant reduction in protein levels, Western immunoblotting was performed on vehicle control and 4MU-treated PTM cells using HAS-specific antibodies (Fig. 1B). After 72 hours of treatment, HAS1 and HAS2 protein levels were significantly reduced by 1 mM 4MU treatment ($P < 0.01$). Although HAS3 levels were also reduced, this did not reach statistical significance.

Silencing lentivirus for each individual HAS was generated and tested for its ability to knock down their respective HAS genes and proteins in TM cells (Fig. 2). By qRT-PCR, HAS1 mRNA levels were reduced by 78% by shHAS1 ($P < 0.0001$), HAS2 mRNA was reduced by 98% by shHAS2 ($P < 0.0001$) and HAS3 was reduced by 72% by shHAS3 lentivirus ($P = 0.035$). By Western blotting and densitometry (Fig. 2B), shHAS1 knocked down 35% of HAS1 protein ($P = 0.01$), shHAS2 knocked down 25% of HAS2 protein ($P = 0.007$) and shHAS3 knocked down 30% of HAS3 protein ($P = 0.01$) as compared to control-infected PTM cells. Representative Western images for each antibody are shown for shCtrl and shHAS-infected TM cells.

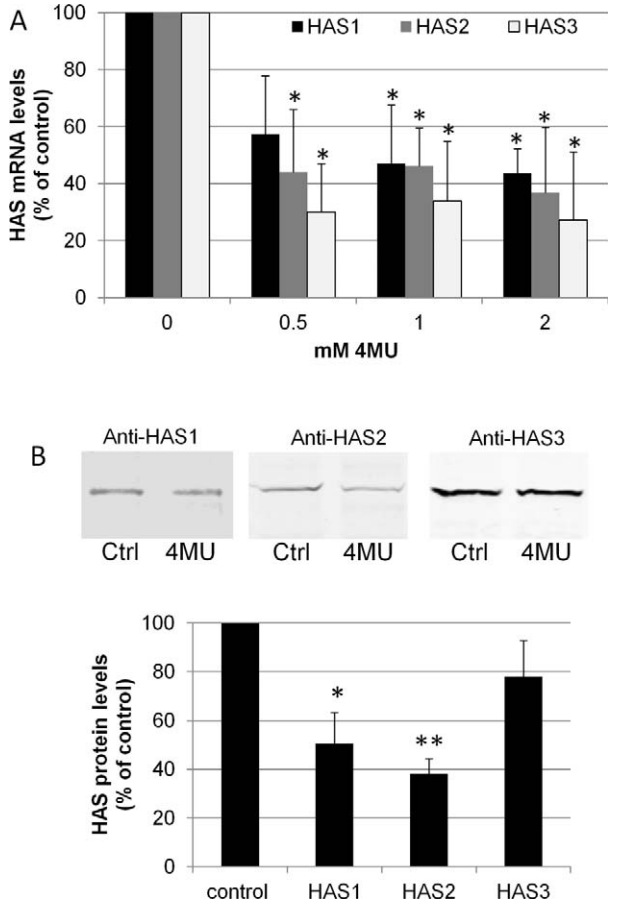

Figure 1. HAS gene and protein levels in PTM cells following 4MU inhibition of HA synthesis. (**A**) Quantitative RT-PCR of HAS1, HAS2, and HAS3 mRNA levels in PTM cells treated for 24 hours with 0.5, 1, and 2 mM 4MU. mRNA levels were normalized to 18S RNA levels and presented as a percentage of the control. $N = 4$ for HAS1 and HAS2 and $n = 3$ for HAS3. * indicates significant change ($P < 0.05$) versus DMSO control by one-way ANOVA. (**B**) Western blots of HASs in control (Ctrl) and 1 mM 4MU treated PTM cells after 72 hours. Densitometry of Western blots showed reduction of HAS protein when normalized to actin. $N = 3$; $^*P = 0.01$ and $^{**}P = 0.0005$ by an unpaired Student's *t*-test, which is significant with Bonferroni correction.

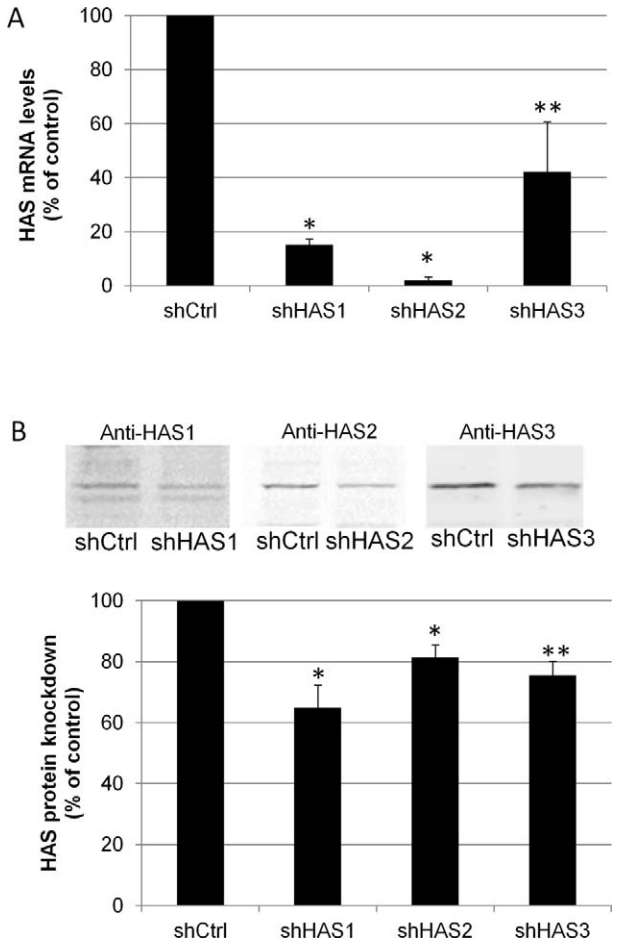

Figure 2. HAS gene and protein levels in PTM cells following HAS gene silencing. (**A**) Quantitative RT-PCR of HAS mRNA levels in PTM cells infected with either shHAS1, shHAS2 or shHAS3 for 5 days. mRNA levels were normalized to 18S RNA levels and presented as a percentage of control shRNA-infected cells. $^*P = 0.0001$ for HAS1 and HAS2 and $^{**}P = 0.035$ for HAS3 by an unpaired Student's *t*-test, $n = 3$. (**B**) Western blots of HASs in shHAS-infected or control-infected (shCtrl) PTM cell lysates. Densitometry of Western blots showed a significant reduction in HAS protein levels when normalized for actin. $N = 3$; $^*P = 0.01$; $^{**}P = 0.006$ by an unpaired Student's *t*-test, which is significant with Bonferroni correction.

HA Concentration by ELISA Assay

To determine whether the reduction of HASs by either 4MU inhibition or gene silencing reduced HA concentration, we performed an HA ELISA assay to quantitate HA levels in TM cell lysates and in the media (Fig. 3). In porcine TM cells (Fig. 3A), there was an approximately 30% to 40% reduction in HA levels in both the cell lysates and media when shHAS1 and shHAS2 were silenced. For shHAS3 silencing, HA levels in the cell lysates were not reduced but HA in the media was reduced approximately 30%. 4MU treatment reduced HA levels approximately 60% to 75% both in the cell lysates ($P = 0.0001$) and media ($P = 0.005$). In human TM cells (Fig. 3B), HA levels were reduced approximately 15% to 20% in the cell lysates and 25% to 30% in the media ($P < 0.008$) when each HAS was individually targeted by gene silencing. In 4MU-treated TM cells, there was an approximately 40% and 60% reduction in HA levels in the cell lysates ($P = 0.05$) and media ($P = 0.0001$), respectively. We also compared the relative percentage of HA in the RIPA lysates and media in control human and porcine TM cells (Fig. 3C). In human TM cells, 22% of HA was present in the cell lysates and 78% was in the media. For porcine TM cells, 5% of HA was present in the cell lysates and 95% was in the media. This represents a significant distribution change with relatively more HA in the pericellular matrix in human TM cells compared to porcine TM cells ($P = 0.0018$). Treatment with 4MU did not affect the relative ratio of HA in the pericellular matrix and media in either species.

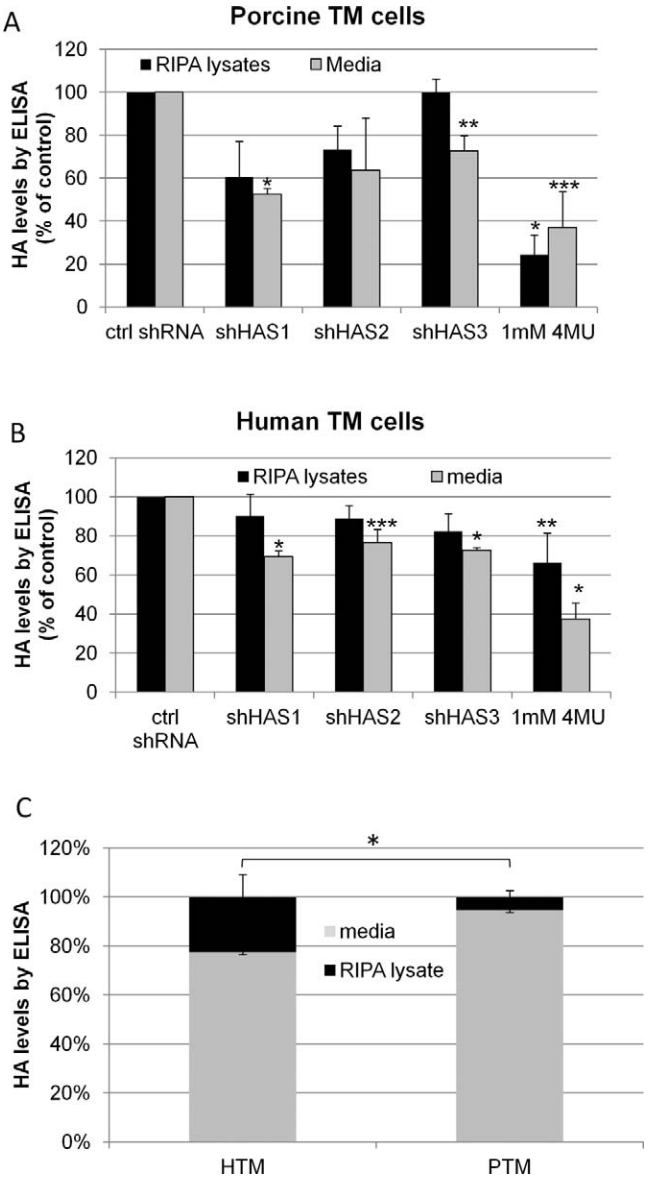

Figure 3. HA concentration in cultured TM cells by ELISA assay. TM cells were infected for 72 hours before serum-free media was applied for 24 hours. 4MU treatments lasted 24 hours. HA concentration in RIPA cell lysates and media was quantitated using a competitive HA ELISA assay. (**A**) HA levels in porcine TM cells. $N = 3$ for shHAS1 and shHAS3, $n = 2$ for shHAS2, $n = 5$ for 4MU. $^*P = 0.0001$; $^{**}P = 0.02$; $^{***}P = 0.005$ by an unpaired Student's *t*-test. (**B**) HA levels in human TM cells. $N = 3$ for shHAS1 and shHAS3, $n = 5$ for shHAS2 and 4MU. $^*P = 0.0001$; $^{**}P = 0.05$; $^{***}P = 0.008$ by an unpaired Student's *t*-test. (**C**) For control cells, the percentage of HA in RIPA lysates and media was compared between human (HTM) and porcine TM (PTM) cells. The proportion of HA in the pericellular matrix was significantly more in human TM cells compared to porcine TM cells. $^*P = 0.0018$ by a two-tailed Fisher exact test; $n = 6$.

Effects of Inhibition of HA Synthesis on Outflow Facility

Next, we investigated the effect of the HA synthesis inhibitor, 4MU, on outflow facility (Fig. 4). This was applied continuously for the duration of the experiment. Outflow facility was decreased by approximately 50% over 158 hours in human eyes (Fig. 4A). Conversely, outflow facility was increased 2.1-fold in porcine eyes after 72 hours of treatment (Fig. 4B). Vehicle control-treated eyes did not show any significant difference in outflow facility for either species.

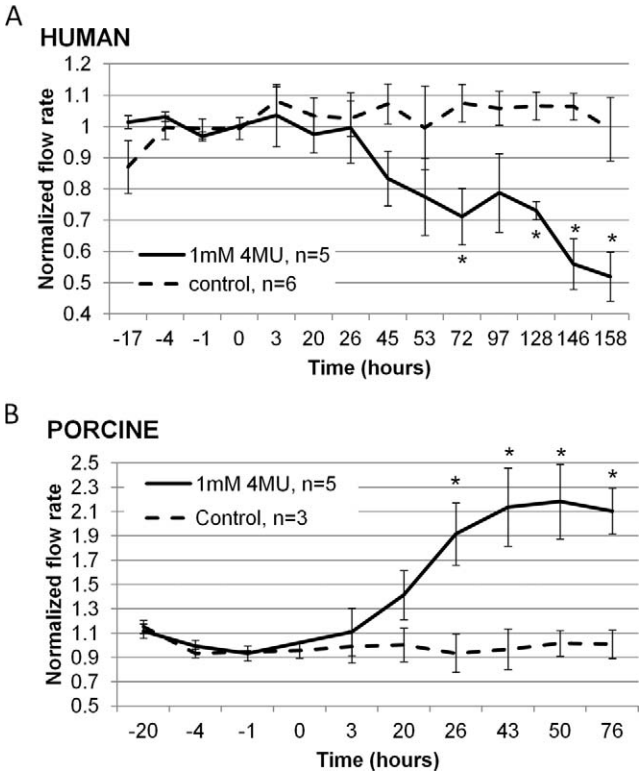

Figure 4. Effects of 4MU treatment on outflow facility in perfusion culture. (**A**) Outflow facility of human eyes treated with 1 mM 4MU (*solid line*) or vehicle control (*dashed line*). (**B**) Outflow facility of porcine eyes treated with 1 mM 4MU (*solid line*) or vehicle control (*dashed line*). The "*n*" is cited with the graph legend. $^*P < 0.04$ compared to vehicle control eyes by ANOVA.

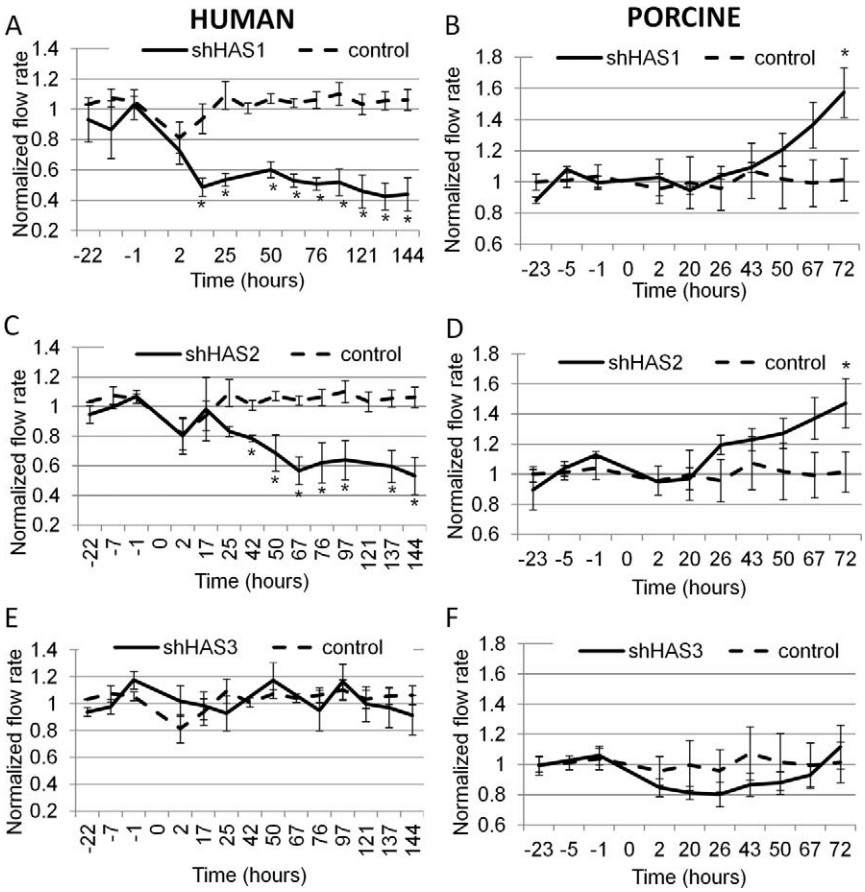

Figure 5. Effects of shHAS gene silencing on outflow facility in perfusion culture. Human (**A**, **C**, **E**) or porcine (**B**, **D**, **F**) anterior segments were perfused with 10^8 pfus of shHAS silencing lentivirus (*solid lines*) or with control lentivirus (*dashed lines*), which was applied at time point 0. (**A**, **B**) shHAS1 silencing, $n = 5$; (**C**) shHAS2 silencing, $n = 5$; (**D**) shHAS2 silencing, $n = 7$; and (**E**, **F**) shHAS3 silencing, $n = 6$. shControl in all human graphs, $n = 4$; shControl in all porcine graphs, $n = 6$. $^*P < 0.04$ compared to control shRNA-infected eyes by ANOVA.

In order to evaluate the individual effects of HAS gene silencing on outflow facility, we applied shHAS lentivirus to human or porcine anterior segment perfusion cultures (Fig. 5). In human eyes, application of shHAS1 lentivirus reduced outflow to approximately 50% at 17 hours after application and to approximately 60% by 144 hours (Fig. 5A). For shHAS2 lentivirus application to human eyes, outflow facility was reduced by 20% at 42 hours and by 50% at 144 hours (Fig. 5C). Conversely, application of shHAS1 and shHAS2 lentivirus to porcine eyes increased outflow facility by approximately 1.5-fold at 72 hours (Fig. 5B, 5D). Interestingly, silencing of HAS3 transcripts did not significantly affect human or pig outflow facility (Fig. 5E, 5F). The same human control data was plotted on each human graph and similarly, the same porcine control data was used on all porcine graphs. The control lentivirus did not affect outflow facility in either species. Representative outflow facility data for 4MU-treated and shHAS-infected human and porcine eyes are shown in the Table.

TM Tissue Analysis Postperfusion

Following perfusion culture, the TM was dissected from the anterior segment, RNA was isolated and qRT-PCR was performed to assess HAS gene expression. HAS mRNA levels following 4MU treatment of human eyes were reduced by 86% for HAS1, 99% for HAS2 and 99% for HAS3 as compared to vehicle control eyes. HAS mRNA levels following shHAS infection of human eyes were reduced by 99% for HAS2 and 94% for HAS3 as compared to control lentivirus-infected eyes by quantitative RT-PCR.

H&E staining was used to assess the gross morphology of the TM post-perfusion in human eyes (Fig. 6). There were no observable structural differences that could not be attributed to sectioning between the control and any of the treated eyes. However, the TM beams of 4MU-treated eyes (Fig. 6D, 6E) appeared slightly less pink (clearer) than control eyes (Fig. 6A, 6B), although the staining of the sclera was a similar shade of pink. HA distribution in TM tissue was detected using bHAbp and Alexa Fluor 594nm-conjugated Streptavidin (Invitrogen).[35,37] Consistent with our previous study,[35] HAbp staining in the TM was somewhat variable. In control eyes, HAbp was concentrated in the JCT region, within 20 μm of Schlemm's canal, in the uveal beams and slightly less surrounding the beams of the corneoscleral meshwork (Fig. 6C). In 4MU-treated human eyes, there was a noticeable decrease in HAbp staining in the JCT region (Fig. 6F). There was also a decrease in HAbp staining in the JCT in shHAS1, shHAS2, and shHAS3-infected TM (Fig. 6I, 6L, 6O).

We also evaluated porcine TM tissue post-perfusion (Fig. 7). Again there were no apparent structural differences between the control and any of the treatments in H&E stained sections. TM cells were readily observable in all sections and there was no apparent disruption of the inner wall of the aqueous plexus. HA distribution, as detected with bHAbp, showed some staining in all sections. In control TM (Fig. 7C), HAbp was found predominantly in the corneoscleral meshwork and the

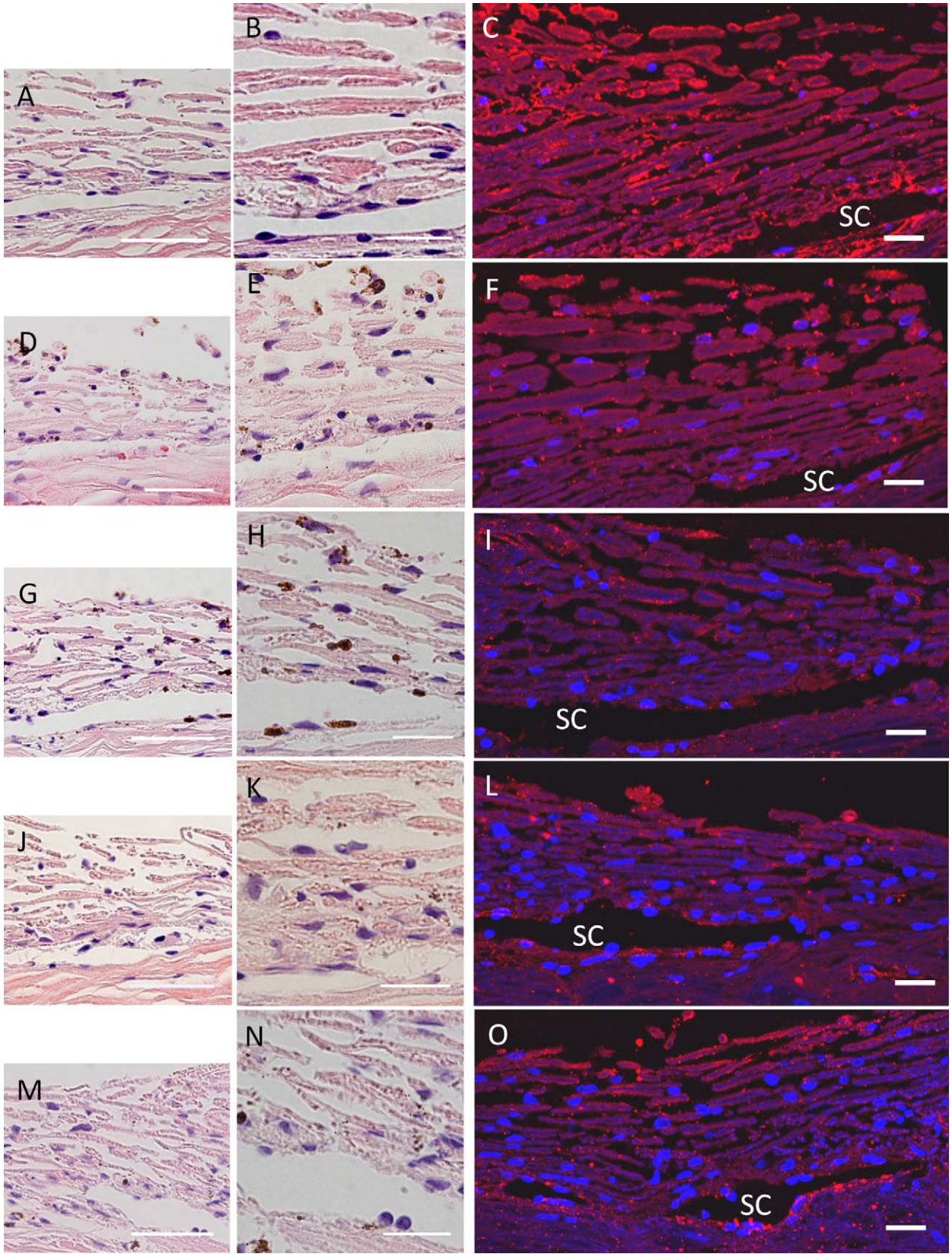

Figure 6. H&E and HAbp staining of human TM tissue. H&E or biotinylated HAbp was used to stain human TM after 144 hours of 4MU treatment or shHAS silencing. HAbp was detected with Streptavidin-conjugated Alexa fluor 594nm (*red*). (**A–C**) shControl; (**D–F**) 4MU-treated; (**G–I**) shHAS1-infected; (**J–L**) shHAS2-infected; and (**M–O**) shHAS3-infected eyes. These images are representative of at least 3 eyes per treatment. SC = Schlemm's canal. DAPI stained the nuclei blue. Scale bars = 50 μm (**A**, **D**, **G**, **J**, **M**); all other images = 20 μm.

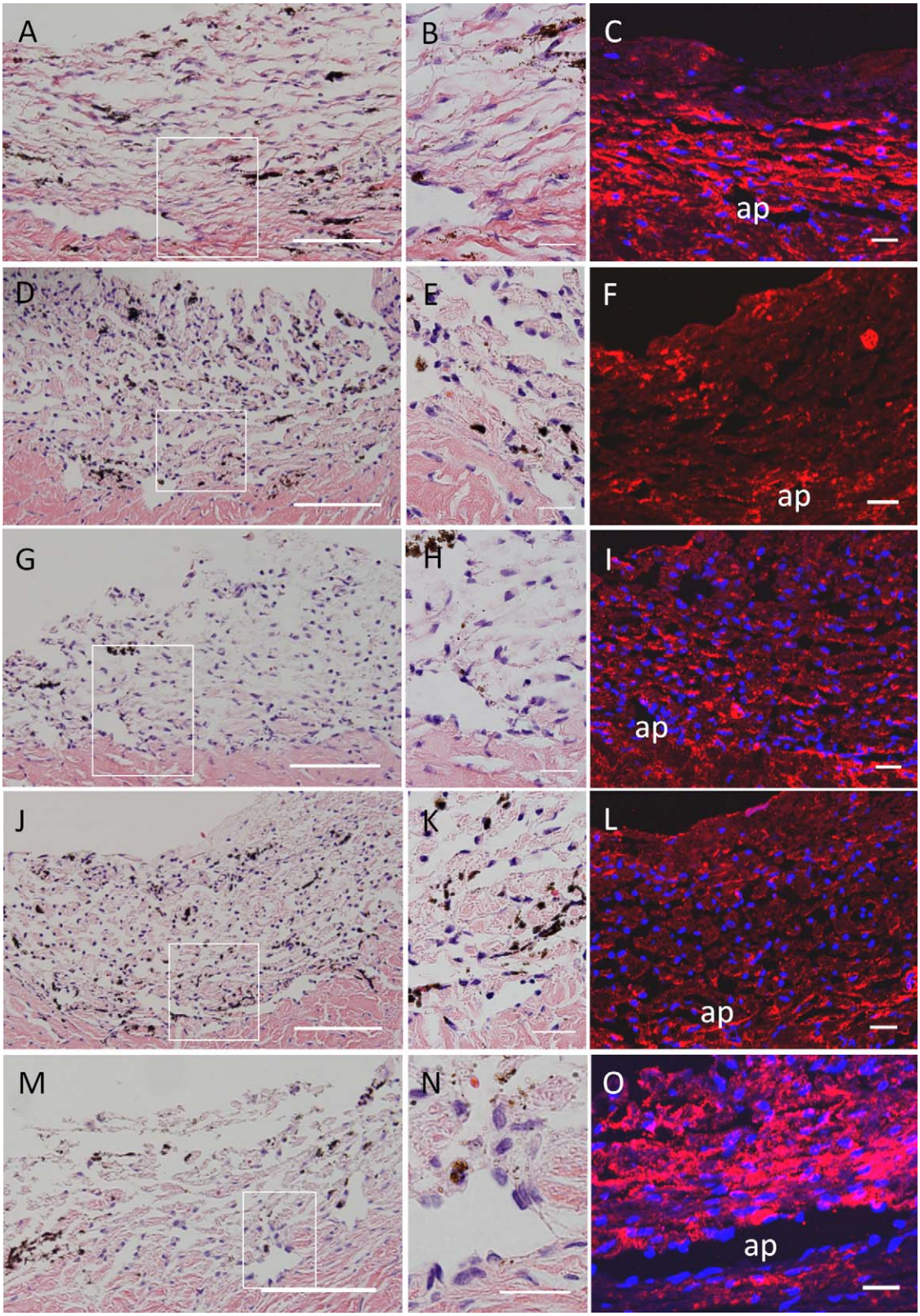

Figure 7. H&E and HAbp staining of porcine TM tissue. H&E or biotinylated HAbp was used to stain porcine TM after 72 hours of 4MU treatment or shHAS silencing. (**A–C**) shControl; (**D–F**) 4MU-treated; (**G–I**) shHAS1-infected; (**J–L**) shHAS2-infected; and (**M–O**) shHAS3-infected eyes. *Boxed area* is shown at higher magnification in **B**, **E**, **H**, **K** and **N**. These images are representative of at least 3 eyes per treatment. Ap = aqueous plexus. Scale bars = 50 μm (**A**, **D**, **G**, **J**, **M**); all others = 20 μm.

Table. Representative Outflow Facility Data for Human and Porcine Eyes Subject to All Treatments

Species	Eye Number	Treatment	Average Flow Rate before Treatment	Flow Rate (μL/min)			
				1 Day	2 Days	3 Days	6 Days
Human	2011-1663OD	Vehicle control	2.14	2.166	2.583	2.418	2.178
Human	2010-0917OD	1 mM 4MU	2.232	2.055	1.189	1.428	1.246
Human	2011-0411OD	shControl	1.397	1.368	1.441	1.261	1.262
Human	2010-1601OS	shHAS1	4.97	2.088	2.934	2.81	2.571
Human	2011-0786OS	shHAS2	1.433	1.075	1.054	1.139	0.906
Human	2011-0789OS	shHAS3	2.815	3.484	3.513	2.743	2.581
Pig	—	Vehicle control	4.821	3.975	3.6666	4.357	—
Pig	—	1 mM 4MU	2.703	4.487	5.513	5.964	—
Pig	—	shControl	3.938	4	3.933	4.103	—
Pig	—	shHAS1	5.135	5.261	7.119	9.225	—
Pig	—	shHAS2	4.199	4.666	5.428	6.097	—
Pig	—	shHAS3	2.598	2.711	3	3.033	—

region next to the aqueous plexus, with much less staining of the uveal beams. There was a large reduction in HAbp staining in 4MU-treated, and shHAS1- and shHAS2-infected eyes (Fig. 7, 7F, 7I, 7L). Reductions were mainly observed in the corneoscleral meshwork and deep in the TM in regions adjacent to the aqueous plexus. HAbp staining of shHAS3-infected eyes showed few differences compared to control TM (Fig. 7O).

Discussion

This study provides strong supportive evidence for a role of HA in outflow resistance in human eyes. In response to 4MU, which inhibits production of all 3 HASs and depletes cellular uridine diphosphate-glucuronic acid,[6,7] an approximately 50% decrease in outflow facility at 158 hours was observed. Moreover, silencing of HAS1 and HAS2 caused similar decreases in outflow facility in human eyes. However, silencing of these individual HASs revealed temporal variations on outflow facility and suggests that HA chains produced by each HAS gene may contribute to outflow resistance in different ways. Silencing of HAS1 showed significant decreases within 17 hours of application of silencing lentivirus to human eyes. shHAS2 also decreased outflow facility in human eyes, but the effects took longer to occur than shHAS1 silencing. This temporal difference between shHAS1 and shHAS2 outflow facility may reflect differences in the activity of each enzyme or could indicate the existence of two pools of HA: HAS1-synthesized HA may have a shorter half-life and higher turnover rate than HAS2-synthesized HA. Nevertheless, it seems that hyaluronan chains synthesized by both HAS1 and HAS2, which are probably high molecular weight forms, are critical for maintenance of outflow resistance in the TM. Knocking down HAS3 did not significantly affect outflow facility. This suggests that HA chains produced by HAS3, which are probably low molecular weight forms, do not contribute significantly to outflow resistance. However, the relative efficacy of the HAS3 knockdown on HA levels was slightly lower, possibly diminishing its effects.

The observed decrease in outflow facility caused by inhibition of HA synthesis in human eyes was opposite to the effects caused by modifiers of other GAG chain types. Previously, we showed that inhibition of attachment of GAG chains to proteoglycan core proteins by β-xyloside, or inhibition of GAG chain sulfation by sodium chlorate, increased outflow facility in both human and porcine eyes.[35] Neither of these treatments would affect HA chains. An increase in outflow facility was also reported for both human and porcine eyes upon RNAi silencing of the ChGn gene, an enzyme that catalyzes the first step in chondroitin sulfate GAG synthesis.[29] Although HA and other GAG chains clearly serve important roles in outflow resistance, the observed opposite effects on outflow facility in human eyes suggest that each type of GAG chain serves separate and unique structural organization functions in the outflow pathways.

Previously, we showed that porcine eyes treated with hyaluronidase increased outflow facility 1.7-fold after 5 hours, but this increase was not sustained.[35] In this study, 4MU treatment was found to increase outflow facility in porcine eyes approximately 2-fold over 76 hours, but there was no initial increase at the early time points. This likely reflects the fact that 4MU inhibits HA synthesis rather than affects turnover. However, these two observations combined suggest that hyaluronidases may initially be released to degrade existing HA when resistance needs to be modified, while HA synthesis may be adjusted to maintain the modified outflow. HA interacts with cell surface receptors such as CD44 and receptor for hyaluronan-mediated motility (RHAMM).[1] These receptors readily respond to changes in amounts and size of cell surface HA and transmit signals intracellularly. Alterations in HA levels, either by changes in degradation or synthesis, may therefore influence cellular signaling pathways. This may in turn influence biosynthesis of other molecules such as versican, which is likely a primary component of the outflow resistance.[29]

Inhibition of HA synthesis caused opposite effects on outflow facility in human and porcine eyes. A similar reciprocal response of outflow facility was observed when versican was silenced.[29] The reason for these opposite effects remains unclear. Porcine eyes are a good substitute for human eyes in perfusion experiments as they are similar in size and shape. However, anatomical differences do exist between the two species, which is mainly confined to the inner TM.[38] There is a continuous Schlemm's canal in human TM whereas porcine TM has an aqueous plexus. However, the elastic network in the JCT region does not exhibit any obvious morphologic differences between porcine and primate eyes.[38] In this study, we show differences in the distribution of HAbp staining between species. In human eyes, HAbp stained the uveal beams, corneoscleral meshwork and JCT region, which is consistent with HAbp distribution observed in a prior study.[13] However, in porcine eyes, HAbp staining was largely absent from the uveal beams, but it strongly stained the corneoscleral meshwork and JCT region. Furthermore, there was an apparent increase in HAbp staining in porcine TM compared to human TM. Thus, anatomic differences, particularly in the JCT region, and variations in HA amounts and/or distribution, as assessed by HAbp staining, may contribute to the opposite

effects on outflow facility. In addition, there are likely differences in the ultrastructural organization of the ECM between species, which were not detected by the methods used in this study.

Another observed difference between porcine and human outflow facility was the temporal response to 4MU treatment. In porcine eyes, outflow facility effects were significant at 26 hours after application compared to 72 hours in human eyes. This could indicate that HA turnover in porcine TM is more dynamic than in human TM, possibly reflecting the relatively younger age of the tissue used. Thus, the use of anterior segments from relatively young and old eyes may have contributed to the reciprocal responses on outflow facility between species. Moreover, the amount of HA in the pericellular matrix varied between species. Cultured human TM cells retained a significantly larger proportion of HA in their pericellular matrix (22%) compared to porcine TM cells (5%). Pericellular HA is critical to establish a pericellular hydrated zone, which is stabilized by HA-proteoglycan interactions.[1,4] These HA-rich areas could cause physical separation of structures and create avenues for aqueous outflow through the TM. Assuming that TM cells in tissues exhibit similar differences in their pericellular matrix HA concentrations, inhibition of HA synthesis may disproportionately affect hydration of the human pericellular matrix and cause drastic effects on aqueous traversing flow pathways in the JCT. This may result in the observed decrease in outflow facility. In porcine eyes, the relative paucity of pericellular HA surrounding TM cells may not be as severely affected by treatments that inhibit HA synthesis. Alternatively, HA may not be as critical in maintaining open outflow pathways in porcine tissue as it is in human TM. However, there also remains the possibility that HA from porcine cells was not as easily solubilized in RIPA buffer as human HA. Nonetheless, differences in pericellular HA concentration may affect outflow resistance in both human and porcine eyes.

Previously, porcine eyes were shown to have a prominent washout effect at 30 mm Hg during the first 6 hours of perfusion culture, but there was minimal washout at 7.5 mmHg.[39] Washout was also observed in another study with a constant flow perfusion system and media containing 1% serum.[38] In our studies, porcine eyes were perfused with serum-free media for 24 hours at approximately 8 mmHg to achieve baseline flow rates. Washout was not detected in this study because of this relatively long-term stabilization procedure and perhaps due to other experimental differences between these studies. Moreover, in our study, any eyes that could not be stabilized at a near constant flow rate were discarded. Thus, washout in porcine eyes likely did not contribute directly to the observed differences in outflow facility between species.

Structurally, there were no gross morphologic differences between 4MU- and control-treated eyes upon H&E staining. This was contrary to our previous report using versican-silencing lentivirus, where there was an apparent increase in hematoxylin staining in the JCT region.[29] However, the TM of 4MU-treated eyes tended to be less pink (clearer) than control eyes. Structures that appear clear by eosin staining are hydrophobic. Consistent with this, treatment with 4MU would reduce the amount of hydrophilic HA and could lead to a more hydrophobic tissue. Previously, we observed that versican, a HA binding protein, had a segmental pattern of expression.[29] HAbp staining of radial sections of high and low flow regions from multiple untreated human eyes did not reveal any consistent pattern of segmental HAbp staining (unpublished observation). However, one potential limitation of this study was that HAbp staining was not performed in high and low flow regions of 4MU-treated or shHAS-infected eyes so may not comprehensively represent HAbp staining. We tried to mitigate this limitation by cutting the entire anterior segment post-perfusion into wedges for paraffin sectioning. All wedges were then assessed in order to provide the most complete picture of HAbp staining around the circumference of each eye. The images shown are the most representative HAbp staining for each treatment.

In conclusion, the data presented here confirm prior studies that implicate a major role for HA in outflow resistance probably as a binding partner for versican. Loss of HA in the JCT may render TM cells incapable of launching a normal homeostatic response to adjust aqueous outflow.[40] The profound reduction of HA concentration in POAG TM[12,19] may leave some POAG patients susceptible directly or indirectly to elevated IOP. Together, these results show that HA concentration needs to be tightly regulated in order for the TM to function normally.

Acknowledgments

The authors thank Ruth Phinney (Lions Eye Bank, Portland, OR) for facilitating the procurement of human donor eyes and Carolyn Gendron (Knight Cancer Institute, Oregon Health & Science University) for paraffin sectioning and histology.

References

1. Toole BP. Hyaluronan: from extracellular glue to pericellular cue. *Nat Rev Cancer*. 2004;4:528–539.
2. Weigel PH, DeAngelis PL. Hyaluronan synthases: a decade-plus of novel glycosyltransferases. *J Biol Chem*. 2007;282:36777–36781.
3. Itano N. Simple primary structure, complex turnover regulation and multiple roles of hyaluronan. *J Biochem*. 2008;144:131–137.
4. Evanko SP, Tammi MI, Tammi RH, Wight TN. Hyaluronan-dependent pericellular matrix. *Adv Drug Deliv Rev*. 2007;59:1351–1365.
5. Itano N, Sawai T, Yoshida M, et al. Three isoforms of mammalian hyaluronan synthases have distinct enzymatic properties. *J Biol Chem*. 1999;274:25085–25092.
6. Kultti A, Pasonen-Seppanen S, Jauhiainen M, et al. 4-Methylumbelliferone inhibits hyaluronan synthesis by depletion of cellular UDP-glucuronic acid and downregulation of hyaluronan synthase 2 and 3. *Exp Cell Res*. 2009;315:1914–1923.
7. Vigetti D, Rizzi M, Viola M, et al. The effects of 4-methylumbelliferone on hyaluronan synthesis, MMP2 activity, proliferation, and motility of human aortic smooth muscle cells. *Glycobiology*. 2009;19:537–546.
8. Usui T, Nakajima F, Ideta R, et al. Hyaluronan synthase in trabecular meshwork cells. *Br J Ophthalmol*. 2003;87:357–360.
9. Rittig M, Flugel C, Prehm P, Lutjen-Drecoll E. Hyaluronan synthase immunoreactivity in the anterior segment of the primate eye. *Graefes Arch Clin Exp Ophthalmol*. 1993;231:313–317.
10. Acott TS, Westcott M, Passo MS, Van Buskirk EM. Trabecular meshwork glycosaminoglycans in human and cynomolgus monkey eye. *Invest Ophthalmol Vis Sci*. 1985;26:1320–1329.
11. Gong H, Underhill CB, Freddo TF. Hyaluronan in the bovine ocular anterior segment, with emphasis on the outflow pathways. *Invest Ophthalmol Vis Sci*. 1994;35:4328–4332.
12. Knepper PA, Goossens W, Palmberg PF. Glycosaminoglycan stratification of the juxtacanalicular tissue in normal and primary open-angle glaucoma. *Invest Ophthalmol Vis Sci*. 1996;37:2414–2425.

13. Lerner LE, Polansky JR, Howes EL, Stern R. Hyaluronan in the human trabecular meshwork. *Invest Ophthalmol Vis Sci*. 1997;38:1222–1228.
14. Lutjen-Drecoll E, Schenholm M, Tamm E, Tengblad A. Visualization of hyaluronic acid in the anterior segment of rabbit and monkey eyes. *Exp Eye Res*. 1990;51:55–63.
15. Acott TS, Kelley MJ. Extracellular matrix in the trabecular meshwork. *Exp Eye Res*. 2008;86:543–561.
16. Johnson M. 'What controls aqueous humour outflow resistance?'. *Exp Eye Res*. 2006;82:545–557.
17. Ueda J, Wentz-Hunter K, Yue BY. Distribution of myocilin and extracellular matrix components in the juxtacanalicular tissue of human eyes. *Invest Ophthalmol Vis Sci*. 2002;43:1068–1076.
18. Gabelt BT, Kaufman PL. Changes in aqueous humor dynamics with age and glaucoma. *Prog Retin Eye Res*. 2005;24:612–637.
19. Knepper PA, Goossens W, Hvizd M, Palmberg PF. Glycosaminoglycans of the human trabecular meshwork in primary open-angle glaucoma. *Invest Ophthalmol Vis Sci*. 1996;37:1360–1367.
20. Cavallotti C, Feher J, Pescosolido N, Sagnelli P. Glycosaminoglycans in human trabecular meshwork: age-related changes. *Ophthalmic Res*. 2004;36:211–217.
21. Barany EH, Scotchbrook S. Influence of testicular hyaluronidase on the resistance to flow through the angle of the anterior chamber. *Acta Physiol Scand*. 1954;30:240–248.
22. Peterson WS, Jocson VL. Hyaluronidase effects on aqueous outflow resistance. Quantitative and localizing studies in the rhesus monkey eye. *Am J Ophthalmol*. 1974;77:573–577.
23. Van Buskirk EM, Brett J. The canine eye: in vitro studies of the intraocular pressure and facility of aqueous outflow. *Invest Ophthalmol Vis Sci*. 1978;17:373–377.
24. Gum GG, Samuelson DA, Gelatt KN. Effect of hyaluronidase on aqueous outflow resistance in normotensive and glaucomatous eyes of dogs. *Am J Vet Res*. 1992;53:767–770.
25. Knepper PA, Farbman AI, Telser AG. Exogenous hyaluronidases and degradation of hyaluronic acid in the rabbit eye. *Invest Ophthalmol Vis Sci*. 1984;25:286–293.
26. Hubbard WC, Johnson M, Gong H, et al. Intraocular pressure and outflow facility are unchanged following acute and chronic intracameral chondroitinase ABC and hyaluronidase in monkeys. *Exp Eye Res*. 1997;65:177–190.
27. Francois J, Rabaey M, Neetens A. Perfusion studies on the outflow of aqueous humor in human eyes. *AMA Arch Ophthalmol*. 1956;55:193–204.
28. Grant WM. Experimental aqueous perfusion in enucleated human eyes. *Arch Ophthalmol*. 1963;69:783–801.
29. Keller KE, Bradley JM, Vranka JA, Acott TS. Segmental versican expression in the trabecular meshwork and involvement in outflow facility. *Invest Ophthalmol Vis Sci*. 2011;52:5049–5057.
30. Pasutto F, Keller KE, Weisschuh N, et al. Variants in ASB10 are associated with open-angle glaucoma. *Hum Mol Genet*. 2012;21:1336–1349.
31. Polansky JR, Weinreb RN, Baxter JD, Alvarado J. Human trabecular cells. I. Establishment in tissue culture and growth characteristics. *Invest Ophthalmol Vis Sci*. 1979;18:1043–1049.
32. Stamer WD, Seftor RE, Williams SK, Samaha HA, Snyder RW. Isolation and culture of human trabecular meshwork cells by extracellular matrix digestion. *Curr Eye Res*. 1995;14:611–617.
33. Keller KE, Kelley MJ, Acott TS. Extracellular matrix gene alternative splicing by trabecular meshwork cells in response to mechanical stretching. *Invest Ophthalmol Vis Sci*. 2007;48:1164–1172.
34. Keller KE, Bradley JM, Acott TS. Differential effects of ADAMTS-1, -4, and -5 in the trabecular meshwork. *Invest Ophthalmol Vis Sci*. 2009;50:5769–5777.
35. Keller KE, Bradley JM, Kelley MJ, Acott TS. Effects of modifiers of glycosaminoglycan biosynthesis on outflow facility in perfusion culture. *Invest Ophthalmol Vis Sci*. 2008;49:2495–2505.
36. Bradley JM, Vranka J, Colvis CM, et al. Effect of matrix metalloproteinases activity on outflow in perfused human organ culture. *Invest Ophthalmol Vis Sci*. 1998;39:2649–2658.
37. de la Motte CA, Drazba JA. Viewing hyaluronan: imaging contributes to imagining new roles for this amazing matrix polymer. *J Histochem Cytochem*. 2011;59:252–257.
38. Bachmann B, Birke M, Kook D, Eichhorn M, Lutjen-Drecoll E. Ultrastructural and biochemical evaluation of the porcine anterior chamber perfusion model. *Invest Ophthalmol Vis Sci*. 2006;47:2011–2020.
39. Yan DB, Trope GE, Ethier CR, Menon IA, Wakeham A. Effects of hydrogen peroxide-induced oxidative damage on outflow facility and washout in pig eyes. *Invest Ophthalmol Vis Sci*. 1991;32:2515–2520.
40. Bradley JM, Kelley MJ, Zhu X, Anderssohn AM, Alexander JP, Acott TS. Effects of mechanical stretching on trabecular matrix metalloproteinases. *Invest Ophthalmol Vis Sci*. 2001;42:1505–1513.